# High Precision Tracking of Un-Tuned Micro-Coils for Real-Time Motion Correction Applications

Melvyn B. Ooi[1], Murat Aksoy[1], Ronald D. Watkins[1], and Roland Bammer[1]
[1]*Department of Radiology, Stanford University, Stanford, CA, United States*

**Introduction:** The ability to track the position of micro radio-frequency (RF) coils using magnetic resonance (MR) (1,2) has been the foundation of several advances in MR-guided intervention (3,4), and more recently in real-time motion correction applications (5,6). In our previous motion correction works (7,8), subjects wore a headband containing three such RF-coil "active markers", *tuned* to the resonant frequency, which tracked the orientation and position of the head during brain MRI.

Since the field in the vicinity of a tuned marker is amplified by several orders of magnitude, it requires RF-blocking circuitry to decouple the RF-transmit and RF-receive stages of the MR experiment. This additional circuitry may be impractical for small-scale marker designs. Additionally, poor RF-blocking will result in local $B_1$-amplification, increasing the effective flip-angle seen near the tuned marker, which can cause unpredictable contrast changes in the MR image, and increased RF-heating. To mitigate these concerns and simplify the active marker design, we propose the use of *un-tuned* markers for real-time position tracking. We demonstrate that the signal received from an un-tuned marker is sufficient for position tracking, with measurement accuracy and precision being comparable to that of a tuned marker.

**Methods:** Experiments were performed on a 3T GE-MR750 scanner ( Milwaukee, WI, USA). Two different markers were manufactured. The tuned marker is a two-turn (~ 4 mm diameter) solenoid inductor, with capacitors for a tuned-and-matched resonant circuit. The un-tuned marker is identical to the tuned marker, but without any capacitors. In the cavity of both solenoids is a glass sphere (~ 3 mm diameter) filled with 10 mM Gd-doped water solution, which is the point-source that is tracked. The markers are attached via transmission line to a custom interface box (Clinical MR Solutions, Brookfield, WI, USA) which then connects to the scanner front-end.

Marker positions are measured using the tracking pulse-sequence described in (4,7). A non-selective RF-pulse ($\theta$ = 10º) is followed by positive gradient-echo projection readouts in three orthogonal directions (tracking resolution = 1 mm, total duration = 15 ms), thereby defining the position of each active marker uniquely in 3D-space. The time signal from each marker is dominated by the frequency, $f$, corresponding to its position, $r$, along the applied gradient, $G_r$, according to: $r = 2\pi f/\gamma/G_r$. Fourier transform of the time signal yields a peak corresponding to the marker's position along the projected axis. A quadratic fit to the magnitude of the peak and two surrounding points is made, yielding sub-millimeter resolution of each marker's position below the raw digital resolution. Spoiler gradients designed to dephase the magnetization in large volumes while preserving signal from the smaller glass spheres are used to isolate the sphere's signal relative to any signal from the subject. To compensate for $B_0$-field inhomogeneities, the tracking pulse-sequence described above is repeated with negative readout gradients (total duration = 30 ms), and the $B_0$-corrected positions calculated by averaging the positions measured from the positive and negative readouts (2).

A standard planar LEGO grid was used to evaluate the accuracy and precision of the marker position-measurements. The grid was secured to the scanner bed at a coronal orientation, and aligned with the X and Z gradient axes. To estimate marker accuracy, each marker was moved to 15 evenly-spaced positions, over a range of [-112 112] mm, along both X and Z axes. To estimate marker precision, the $B_0$-corrected tracking pulse-sequence was repeated 10 times at each position. The distance from each MR measurement to a reference point at the center of the grid was calculated. The resulting set of mean MR-measured distances at each position ($D_{MR}$) were compared with corresponding distances measured by digital caliper ($D_{known}$) at the same marker positions. The experiment was repeated using both un-tuned and tuned markers (300 position measurements per marker). Due to similarity of the physical X and Y gradients, behavior in Y was not investigated.

**Fig. 1. Marker Signal**

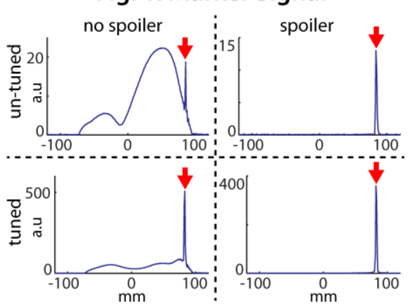


**Fig. 2. Marker Accuracy**

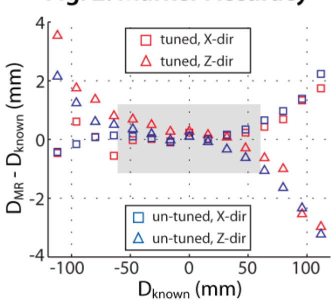


**Fig. 3. Marker Precision**

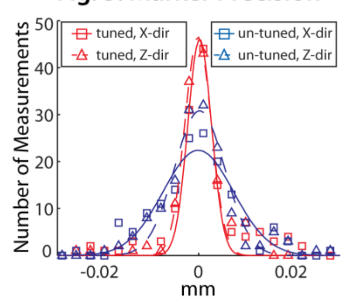


**Fig. 4. Summary**

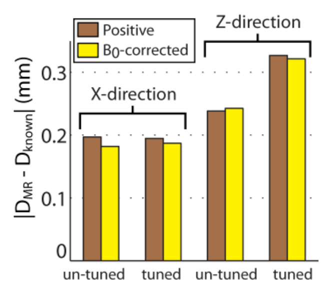


**Results:** Fig. 1 shows the signal from both un-tuned (row 1) and tuned (row 2) markers during a single projection readout, acquired without (column 1) and with (column 2) spoiler gradients. Due to the decreased signal from the un-tuned marker, spoiler gradients are necessary to isolate the marker peak (red arrow) from the background phantom signal. Marker accuracy plots in Fig. 2 show measurement error ($D_{MR} - D_{known}$) of the $B_0$-corrected positions across the full range of the LEGO grid. To evaluate marker precision, the difference between each MR-measurement and its corresponding mean value $D_{MR}$ was calculated; Fig. 3 plots these histogram distributions for the $B_0$-corrected data, which are closely approximated by a Gaussian fit with SD ~ 7µm and 3µm for the un-tuned and tuned markers, respectively. Fig. 4 summarizes the absolute error along the X and Z gradient directions, averaged over all positions within the shaded area in Fig. 2. This area was chosen to approximate the tracking region-of-interest for brain MRI, and to provide a more realistic representation of marker accuracy by separating out the measurement error due to gradient non-linearity (not corrected for in this study). Positions from both the positive readout gradients only, as well as the $B_0$-corrected data, are shown.

**Discussion & Conclusion:** Despite a 5 to 10-fold decrease in SNR between tuned and un-tuned markers, the peak signal from the un-tuned marker is clearly visible for position tracking (Fig. 1, row 1, column 2). Marker precision while twice as large for un-tuned vs. tuned coils (Fig. 3), as expected due to the decrease in SNR, is still on the order of µm. Marker accuracy is comparable between un-tuned and tuned markers (Fig. 2,4). The primary source of error is gradient non-linearity at the outer edges of the LEGO grid (Fig. 2), and was greater in the Z vs. X direction. For brain MRI, motion of the head is physically limited by the imaging coil confines, and so the markers need only be accurate within a smaller region around isocenter (shaded area in Fig. 2). For example, within the range X = [-70 70] mm and Z = [-50 50] mm, accuracy of the un-tuned marker using positive readouts only is (mm, mean ± SD) 0.20 ± 0.14 and 0.24 ± 0.16 along X and Z, respectively. For the full range of grid positions, $B_0$-correction did not significantly improve marker accuracy (Fig. 4), suggesting that tracking using positive readouts alone is sufficient. For applications where tracking is performed beyond this range such as MR-guided intervention, $B_0$-correction and gradient non-linearity compensation will become more critical.

Un-tuned markers, which simplify coil design and reduce undesirable RF-related effects, are a viable option for real-time position tracking applications. Rapid, high-precision, position measurements have been demonstrated, and will find utility in future motion correction studies.

**References:** [1] Ackerman J et al., Proc. 5th ISMRM 1986;1131-32. [2] Dumoulin CL et al., MRM 1993;29(3):411-15. [3] Zhang Q et al., MRM 2000;44(1):56-65. [4] Krueger S et al., IEEE Trans Med Imaging 2007;26(3):385-92. [5] Derbyshire JA et al., JMRI 1998;8(4):924-32. [6] Krueger S et al., Proc. 14th ISMRM 2006; 3196. [7] Ooi MB et al., MRM 2009;62(4):943-54. [8] Ooi MB et al., MRM 2011;66(1):73-81. **Acknowledgements:** This work was supported in part by the NIH (5R21EB006860, 1R01EB011654), the Center of Advanced MR Technology at Stanford (P41RR09784). We also thank Ralph Hashoian, Mina Makram, Phillip Rossman, Ajit Shankaranarayanan, and Gary Glover.